

Contents lists available at ScienceDirect

Journal of Constructional Steel Research



Resilient welded steel moment connections by enhanced beam buckling resistance



Machel L. Morrison *, Tasnim Hassan

Department of Civil, Construction and Environmental Engineering, North Carolina State University, Raleigh, NC, USA

ARTICLE INFO

Article history: Received 9 January 2016 Received in revised form 1 July 2016 Accepted 12 July 2016 Available online 30 July 2016

Keywords:
Steel moment connection
Seismic performance enhancement
Beam plastic hinge
Heat-treated beam section
Web reinforcement

ABSTRACT

This study develops two (2) simple but effective techniques for enhancing buckling resistance of welded steel moment connections (WSMCs). The ANSI/AISC 358-10 prequalified connections satisfy the 4% interstory drift requirement, however experimental studies have shown that their strength degradation may initiate as early as 3% drift. This strength degradation has been observed to be initiated by buckling of the beam web which is followed by buckling of the beam flange and twisting of the beam. Consequently, buildings with the prequalified connections may sustain significant buckling damages under severe earthquakes and it is questionable as to whether these connections are capable of resisting gravity loads or lateral loads from strong aftershocks following a severe earthquake. To improve upon these shortcomings, two (2) performance enhancing techniques are proposed and investigated through finite element analysis (FEA). The more promising of the two involves reinforcing the beam web in the expected plastic hinge with a web reinforcement plate. Finite element analysis demonstrated that this reinforcement enhances the beam buckling resistance of WSMCs and thereby significantly reduces the beam buckling damages even at 5% interstory drift. The potential of this technique is analytically and experimentally demonstrated for the recently developed heat-treated beam section (HBS) WSMC. Test results confirm that the web reinforcement plate was effective in reducing local buckling damage and associated strength degradation, thereby improving the performance of HBS WSMCs. Areas for application and future development of the proposed techniques are identified.

© 2016 Elsevier Ltd. All rights reserved.

1. Introduction

More than a decade of research activities after the Northridge and Kobe earthquakes has developed modified designs of welded steel moment connections (WSMCs) with improved ductility [1]. By eliminating premature weld or near weld failures the current moment connections pregualified for special and intermediate moment frames (SMF and IMF) by the ANSI/AISC 358-10 [2] have demonstrated the ability to attain at least 4% interstory drift while sustaining 80% of the nominal flexural strength (M_D). However, the ANSI/AISC 314-10 Seismic Provisions [3] notes that while connection qualification emphasizes plastic rotation capacity, the tendency for connections to experience strength degradation is of concern as this strength degradation can increase rotational demands from P-delta effects and adversely affect frame stability. In reported studies [4–8], prequalified connections such as the welded unreinforced flange-welded web (WUF-W), reduced beam section (RBS), extended end plate (EEP), bolted flange plate (BFP) and Kaiser bolted bracket (KBB) experience severe strength loss due to beam buckling prior to the termination of loading. Due to this rapid strength loss, frame stability may be jeopardized in a severe earthquake and it

is questionable whether these connections are capable of resisting gravity loads or strong aftershocks following such an event.

The majority of research efforts on the seismic performance of WSMCs have focused on circumventing weld or near weld failures which limited the attainable plastic rotation of these connections during the Northridge Earthquake [1]. However some research has been conducted on local beam buckling failures and the associated strength loss during seismic loading [9–11,13,15–17]. The following is a brief review of the findings of research studies conducted to either improve understanding of the local buckling failure modes of WSMCs or to prescribe and evaluate techniques to improve the resistance of WSMCs to such failures.

Yu et al. [9] collected experimental data on the local buckling modes that result in strength loss in RBS connections. Selected results from their test of an all welded RBS connection with a W30 \times 99 beam connected to a W14 \times 176 column are shown in Fig. 1a. For details of the experimental setup, loading history, instrumentation etc. the reader is referred to the research report from the study [9]. In Fig. 1a, the envelope of the applied load and measured buckling amplitudes are shown to illustrate the progression of local beam buckling and its effect on connection strength loss. These results indicate that web local buckling (WLB) and lateral torsional buckling (LTB) are initiated early in the loading history (between 1 and 2% drift in the RBS region). It is noted

^{*} Corresponding author.

E-mail address: mlmorris@ncsu.edu (M.L. Morrison).

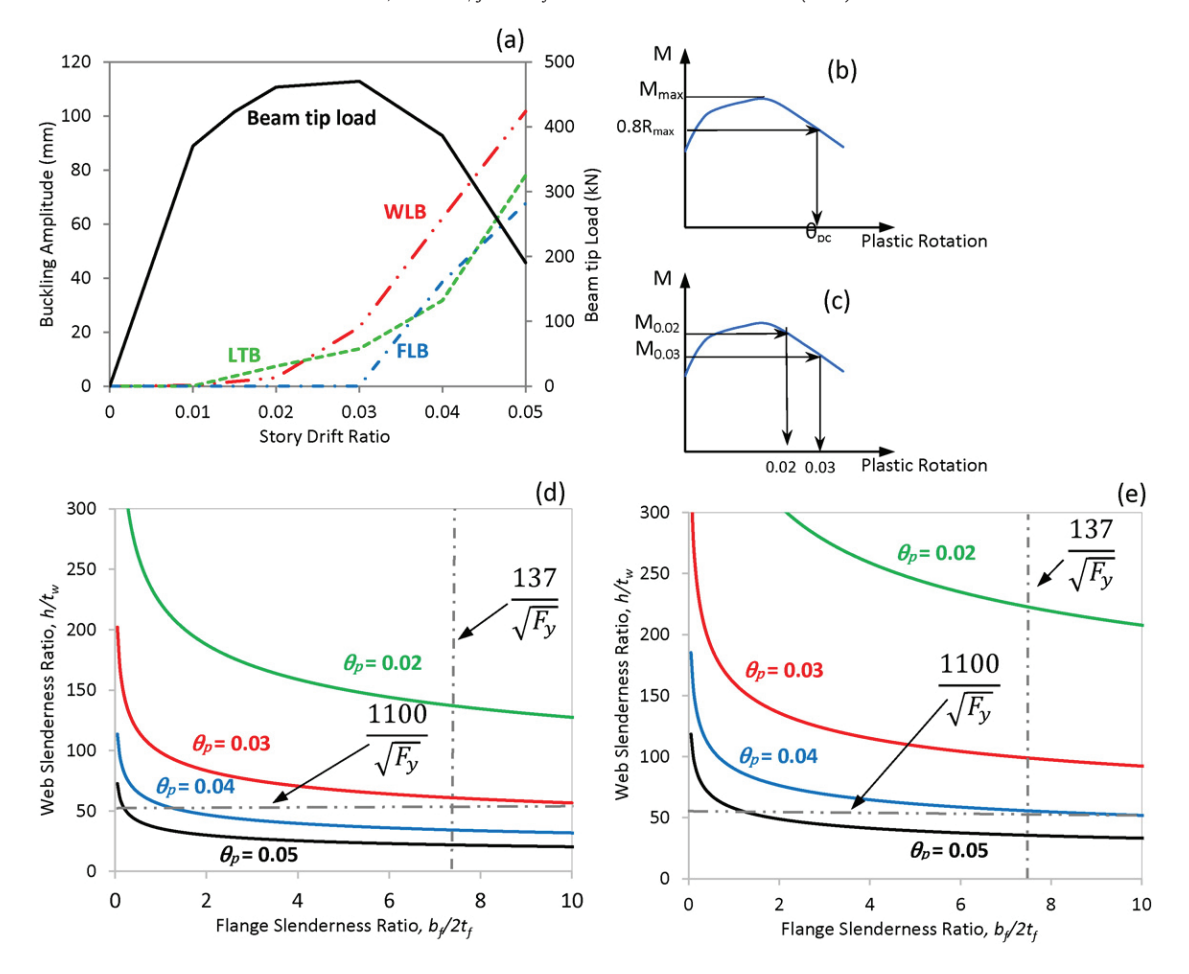


Fig. 1. (a) Measured local buckling modes and strength degradation of a RBS beam to column moment connection (Data from Yu et al. [9]) (b) Definition of plastic rotation capacity by Uang and Fan [10] (c) Definition of strength degradation ratio by Uang and Fan [10] (d) Limiting Slenderness Surfaces for RBS beam to column moment connections (F_y =345 MPa) [10] (e) Limiting Slenderness Surfaces for RBS beam to column moment connections (F_y =223 MPa) [10].

that in RBS connections, the beam flanges are trimmed to relocate plastic hinging of the beam away from the column face to the reduced section and as a result, the largest bending stresses in the beam web occur in the reduced section. In this region, the beam web experiences less rotational restraint along its vertical edge (adjacent to the column flange) and along its horizontal edge (adjacent to the beam flange). Therefore, although trimming of the beam flanges improves flange compactness at the center of the reduced section, it increases the susceptibility of the beam to WLB. Yu et al. [9] also evaluated the effect of a near fault loading history and the addition of lateral bracing near the reduced section on the response of RBS moment connections through full scale experiments. The study showed that additional lateral bracing near the RBS region did not delay the onset of strength degradation but did slow the rate of strength degradation. Finally, finite element analysis reported in this study showed that axial restraining effects from the columns in a frame system can also reduce strength degradation rates for RBS moment connections.

Uang and Fan [10,11] examined the stability criteria for steel moment connections with reduced beam sections through nonlinear regression based on the test results of 55 full-scale RBS moment connections. In their study, connection resistance to buckling induced strength degradation was quantified by

1. The plastic rotation capacity (θ_{pc}) , defined as the total plastic rotation beyond which a connection starts to degrade below 80% of the peak strength (Fig. 1b). Plastic rotation is calculated by dividing the plastic component of the beam tip displacement by the distance from the beam tip to the column centerline.

The strength degradation rate (SDR) defined as the ratio of connection resistance (bending moment) at 0.03 and 0.02 rad plastic rotation (Fig. 1b).

By studying the statistical influence of flange slenderness ratio ($b_f/2t_f$), web slenderness ratio (h/t_w), slenderness associated with LTB (L_b/r_y), and yield strength (F_y) on connection plastic rotation capacity (θ_{pc}), the following equation was developed by Uang and Fan [10,11] to describe the relationship between these parameters:

$$\theta_{pc} = 5.8 \left(\frac{b_f}{2t_f} \right)^{1/8} \left(\frac{h}{t_w} \right)^{1/2} \left(F_{ye} \right)^{1/2}$$
 (1)

where b_f is the beam flange width, t_f is the beam flange thickness, h is the clear distance between beam flanges less the fillet radius for rolled shapes, t_w is the beam web thickness, L_b is the unbraced beam length, r_y is the radius of gyration about the y-axis, and F_{ye} is the expected yield stress defined as:

$$F_{\nu e} = R_{\nu} F_{\nu} \tag{2}$$

where R_y is the ratio of expected yield stress to specified minimum yield stress

Eq. (1) was developed using the unreduced section properties. This equation does not include the LTB slenderness ratio (L_b/r_y), as LTB was not found to have much effect on the plastic rotation capacity of connections in the data set examined [10,11]. Note the relatively stronger influence of the web slenderness ratio (h/t_w), as compared to flange

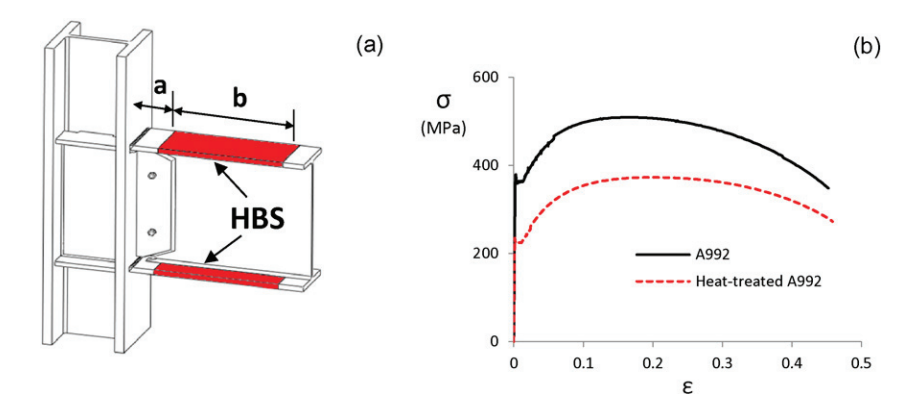


Fig. 2. (a) Sketch of heat-treated beam section (HBS) connection [20] (b) engineering stress-strain response of A992 and heat-treated A992 steel [20].

slenderness ratio ($b_f/2t_f$) predicted by the equation. This strong influence of web slenderness ratio on plastic rotation capacity was discussed in detail by Uang and Fan [10,11] who recommended a web slenderness limit of $1100/\sqrt{F_y}$ to ensure that connections are capable of achieving at least 0.03 rad plastic rotation. This limit was later adopted in the ANSI/AISC 341-02 *Seismic Provisions* [12].

The limiting surfaces for various plastic rotation capacities based on Eq. (1) assuming grade 50 steel F_y = 345 MPa and R_y = 1.1 are plotted in Fig. 1d, while the corresponding limiting surfaces assuming F_y = 223 MPa and R_y = 1.1 are plotted in Fig. 1e. (Fig. 1e will be discussed in more detail later). The limiting flange and web slenderness ratios

for highly ductile members given in the ANSI/AISC 341-10 *Seismic Provisions* are shown in vertical and horizontal dashed lines in Fig. 1d. As shown in the figure, conformance with these limits results in a connection capable of attaining a plastic rotation capacity of 0.03 rad for grade 50 steel. Assuming an elastic connection rotation of 0.01 rad, connections that satisfy these slenderness ratio limits should be capable of achieving 0.04 rad total rotation or 4% drift with no greater than 20% strength loss which is the prequalification criteria for connection use in special moment frames [3]. Uang and Fan [10,11] also showed that the concrete slab reduces the rate of strength degradation due to beam buckling under positive bending but not under negative bending.

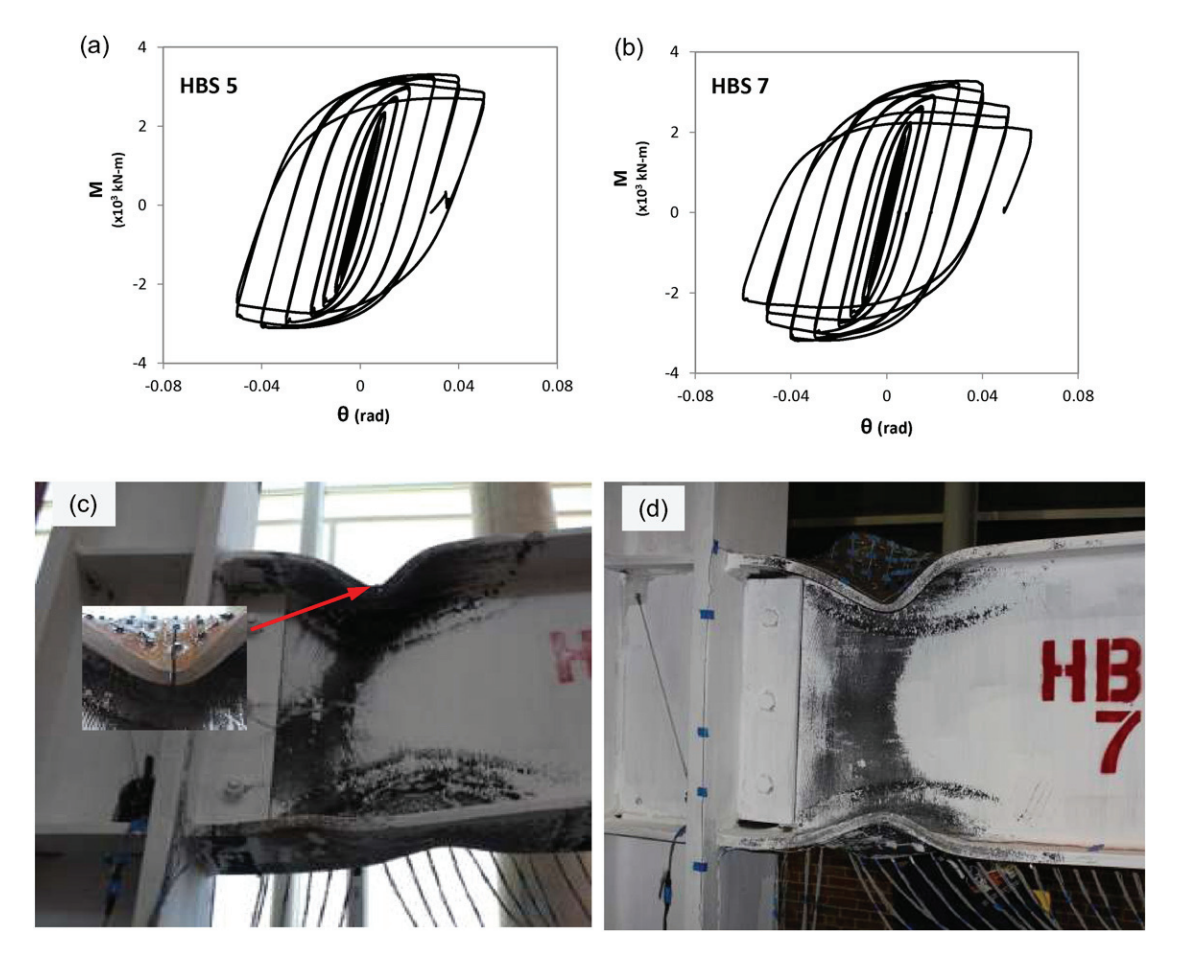


Fig. 3. Test results of HBS 5 and HBS 7 WSMCs, (a) HBS 5 moment-rotation response [20] (b) HBS 7 moment-rotation response [20] (c) photograph showing HBS 5 beam flange buckling and fracture at the crest of flange buckle (d) photograph showing plastic hinge formation and significant beam flange buckling of HBS 7.

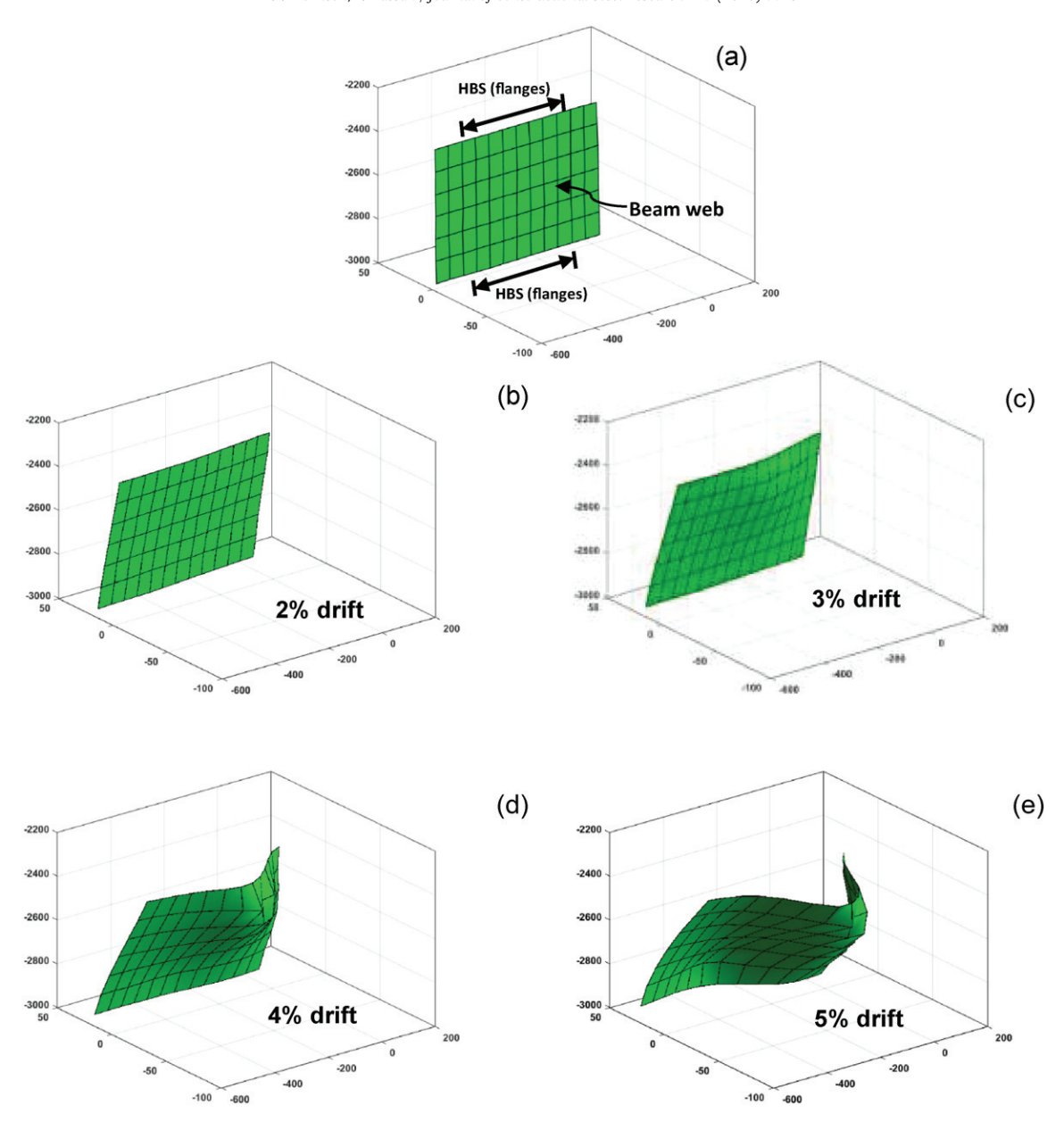


Fig. 4. Progression of buckling in beam web of HBS 5 at various stages of loading history (a) initial position (b) 2.0% drift (c) 3.0% drift (d) 4.0% drift (e) 5.0% drift (Beam is in positive bending i.e. top flange in compression).

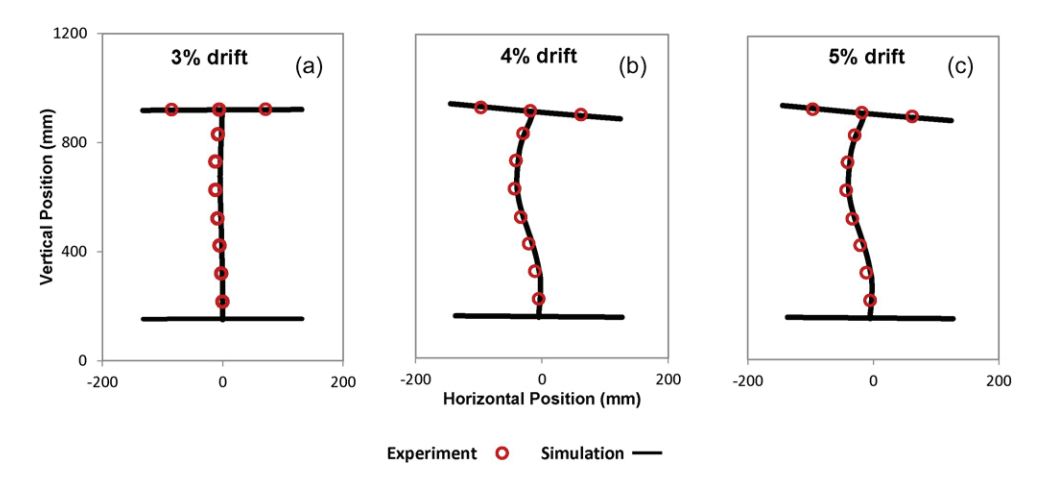


Fig. 5. Progression of HBS 5 beam cross-section buckling at interstory drifts, (a) 3%, (b) 4%, and (c) 5%. Cross-section is located 406 mm from the column face, the beam is in positive bending and FE simulation predictions are plotted against recorded data from test.

Therefore, additional bracing from the concrete slab cannot be relied upon to effectively mitigate strength degradation due to local beam buckling under load reversals.

Okazaki et al. [13] combined finite element analysis (FEA) with the nonlinear regression techniques used by Uang and Fan [10,11] to study lateral torsional and local buckling of beams subjected to cyclic loads. The results of their study showed there to be an interaction between both flange and web slenderness parameters on the strength loss of moment connections due to buckling. The study also found that the stability requirements of the AISC 341-05 Seismic Provisions [14] were adequate to maintain 80% of the nominal beam plastic moment $(M_{\rm p})$ at a story drift of 0.04 rad.

The afore described studies have mainly focused on improving the understanding of the local buckling failure modes of beam to column moment connections during seismic loading, however, some attempts have also been made to delay the onset and slow the rate of strength degradation due to buckling by various reinforcing methods. Kim et al. [15] identified web local buckling as a trigger for strength degradation in their cyclic tests of welded cover plate connections. As a result, they tested one welded cover plate specimen in which two pairs of horizontal stiffeners were welded to the beam web approximately one quarter of the beam depth from the top and bottom flanges in the expected plastic hinge region. While this may seem in concept to be a relatively simple and economical method to delay the onset of strength degradation without significantly increasing the strength of the connection, test results showed that the stiffeners did not delay the initiation of strength degradation. As a result, Kim et al. [15] recommended reduction of web slenderness limits for beams designed for seismic use as opposed to adding web stiffeners.

Wang et al. [16] also used horizontal web stiffeners on all-welded (welded flange-welded web) built-up non compact beams to delay the onset of strength degradation due to buckling. These stiffeners were shop welded to the beam web and column flange on both sides of the beam web in the anticipated plastic hinge region. Improvement in delaying the onset of strength degradation was obtained when two pairs of stiffeners located one third of the beam depth from the top and bottom flanges were used in lieu of one stiffener attached at the beam centerline. However, this method is not suitable for typical WSMC construction practice in the United States where beams are usually field welded to columns with bolted shear tabs because the bolted shear tabs obstruct the attachment of the horizontal stiffeners on one side of the beam web.

Li et al. [17] evaluated the local buckling of moment connections with RBS beams subjected to cyclic loading using FEA. The study showed that, similar to the findings of Yu et al. [9] supplemental lateral bracing near the reduced beam section provided only a modest improvement in local buckling resistance. Therefore, the use of vertical stiffeners attached to the beam web and beam flanges in the reduced section was investigated as a local buckling mitigation technique. This

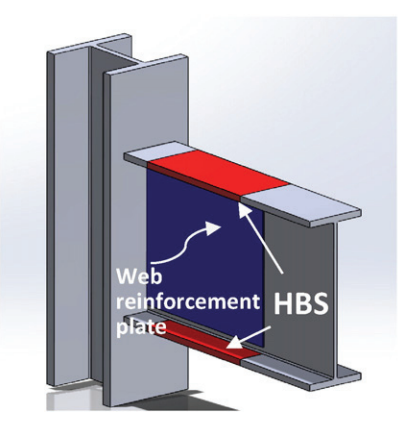
investigation revealed that the use of two or three stiffeners placed equidistant from each other in the reduced section delayed the onset and slowed the rate of strength degradation. However, it was also discovered that the maximum stress within reduced section was increased by 25% due to the addition of the stiffeners. This was found to be the result of stress concentrations that tend to accompany the attachment of transverse stiffeners. In previous studies [18,19] stress concentrations from the attachment of vertical stiffeners were found to be the cause of premature fractures when placed in regions that experience large inelastic strains. Hence, despite its attractive features (effective in reducing strength degradation due to buckling, while being relatively simple to fabricate and install) transverse stiffeners may not be a feasible option.

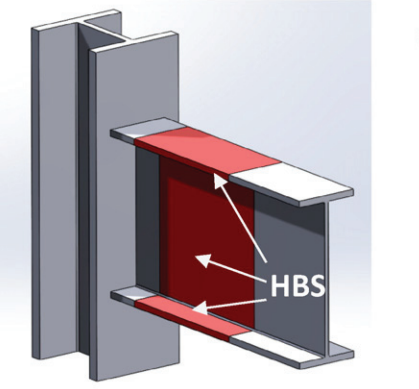
In several of the afore-described studies [10,11,13,15], WLB in the plastic hinge has been observed to play a strong role in the initiation and progression of connection strength degradation. This has been found to be the case especially when connections are designed for beam plastic hinging (as opposed to panel zone shear distortion) to dominate the inelastic behavior. This form of instability (WLB) is expected due to the deep beams (with slender webs) tested in lab experiments and is more closely related to the geometry of the beam rather than the connection method and details. This strong influence of WLB on strength degradation has also been observed during testing of a recently developed WSMCs involving a novel concept called heat-treated beam section (HBS) [20,21]. The study presented in this article will examine local buckling and the associated strength degradation mechanism observed during full scale testing of HBS connections. From this analysis, two (2) strategies to enhance the buckling resistance of allwelded HBS connections are proposed and studied numerically through finite element analysis (FEA). The more promising strategy is experimentally validated through full scale simulated seismic testing. The experimental results from testing of the prototype specimen are analyzed and compared to experimental results of otherwise identical HBS connections to demonstrate the enhanced performance obtained from the proposed technique. Details of the experimental study are presented and areas for future development and application of the proposed techniques are identified.

2. Buckling of recently developed seismically resilient WSMCs

The heat-treated beam section (HBS) WSMC has been recently developed and validated in other studies [20,21], however, for convenience a brief description of the HBS concept and application is presented here. This brief description is followed by a presentation of experimental data from recently tested HBS WSMCs demonstrating HBS seismic performance and local buckling strength degradation mechanism

In HBS connections, specific locations of the top and bottom beam flanges are heated to a temperature in the range of 1050–1100 °C for





(b)

Fig. 6. Proposed enhanced connections (a) HBS with web reinforcement plate (HBS-WR) (b) HBS applied to beam flanges and beam web (HBS-W).

(a)

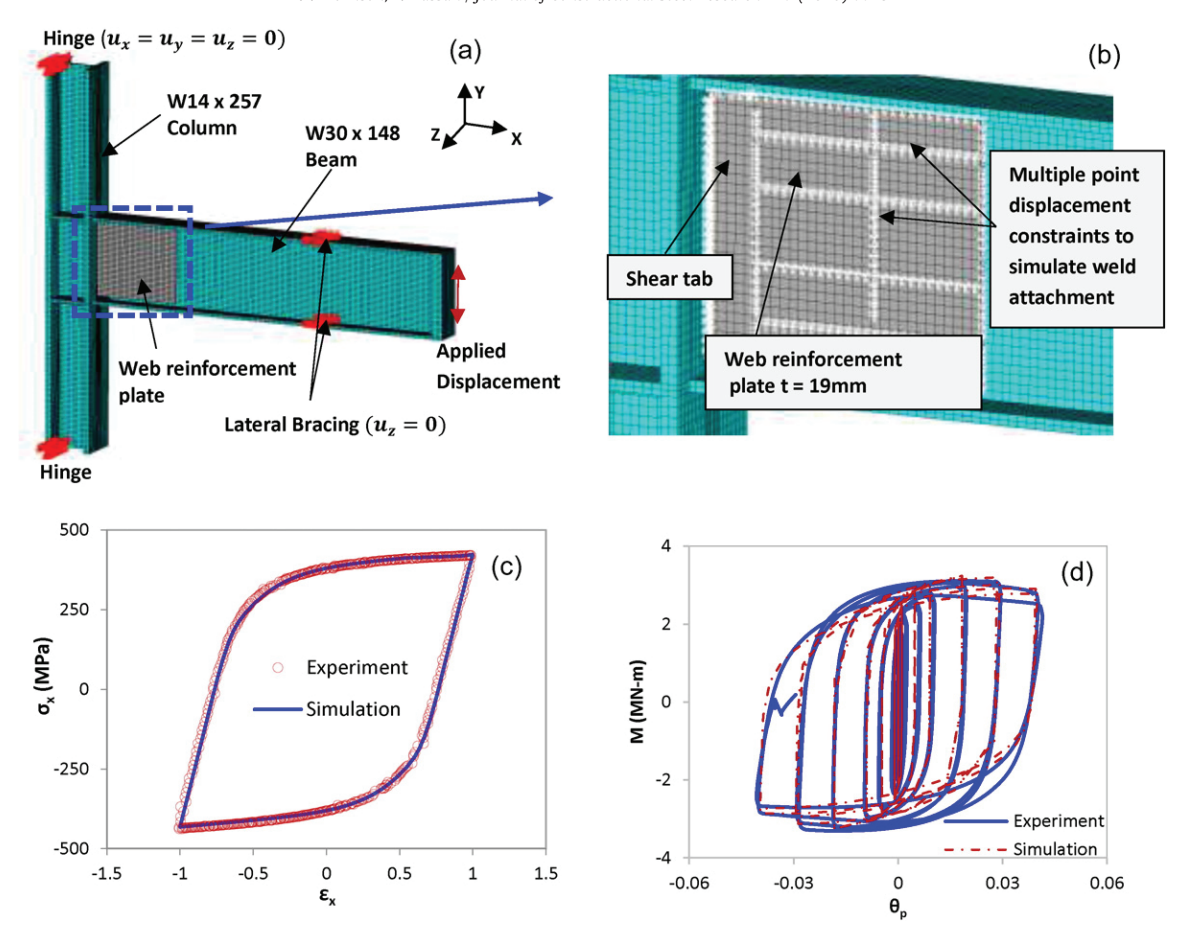


Fig. 7. (a) FE mesh and boundary coditions of HBS-WR (b) Close up view of mesh showing multi-point displacement constraints used to simulate welding attachment of the web reinforcement plate to beam web (c) fitted ASTM A992 hystersis curve (d) comparison of experiment and simulated moment-plastic rotation responses of HBS 5.

15 min followed by slow cooling [20]. The heat-treated areas are highlighted red in Fig. 2a which show the HBS applied to an all-welded connection. This heat treatment reduces the strength of A992 steel as shown in Fig. 2b. As a consequence of this strength reduction, plastic hinging of the beam takes place in the heat-treated beam section (HBS). In a similar manner to the RBS, this connection provides a ductile seismic fuse through weakening, but because the elastic modulus of the heat-treated steel is unchanged, a connection modified with such a technique does not sacrifice elastic stiffness as does the RBS [20]. Note that HBS geometric parameters "a" which corresponds to the distance from the face of the column flange to the beginning of the HBS and "b" which corresponds to the length of the HBS (Fig. 2a) may be chosen similar to RBS parameters "a" and "b" [20].

The moment-rotation responses shown in Fig. 3a and b demonstrate the seismic performance of identical all-welded HBS connections (HBS 5 and HBS 7 respectively) which exceeds current AISC 341-10 seismic provision [3] requirements for use in SMFs. These global responses of HBS connections show wide hysteresis loops indicating good energy dissipation. Strength degradation due to excessive local web, flange and lateral torsional buckling initiated during the 2nd cycle of loading at 4% drift and continued during later loading cycles (see Fig. 3a and b). Loading of HBS 5 was terminated after sustaining 2 loading cycles at 5% drift due to a fracture in the location of significant flange buckling (see Fig. 3c) while loading of HBS 7 was terminated due to significant strength loss resulting from beam buckling (see Fig. 3d).

To demonstrate the progressive strength degradation mechanism of HBS WSMCs 3-dimensional and 2 dimensional plots (Figs. 4 and 5) of displacement measurements from LED sensors placed on the beam flange and web of HBS 5 [20] are presented. In Fig. 5, FE simulations are compared to the experimental responses and will be discussed in

more detail later. From these plots, local buckling of the beam web within the HBS is clearly noticeable at 3% drift (Figs. 4c and 5a). This beam web buckling was also visually observed at this stage in the loading history. At this same point in the loading history, flange buckling was neither observed visually nor detected by LED sensor displacement measurements (Fig. 5a) [20]. This indicates that similar to the RBS connection tested by Yu et al. [9] (Fig. 1a), web buckling precedes flange buckling in HBS connections with this geometric configuration. During the first excursion to 4% drift, beam flange buckling became noticeable (Fig. 5b). As loading progressed, beam flange and web buckling amplitudes continued to increase as shown in Fig. 4d, by 5% drift, severe twisting of the beam web is noticeable (Figs. 4e and 5c) as well as double curvature from buckling during loading in the opposite direction (negative bending).

This buckling damage is similar to those observed in previously studied WSMCs like the RBS and WUF-W [9,4] and have also been observed in other connections modified with the HBS [21]. In other words, the buckling damage discussed above for HBS beams is not induced because of the material strength reduction from the heat treatment or by the connection method, but it is a characteristic behavior of the wide flange cross section.

3. Proposed techniques for enhancing beam buckling resistance of WSMCs

Based on the observed influence of WLB on the initiation of the strength degradation mechanism of HBS (and other WSMCs), two (2) techniques to improve the local buckling resilience of HBS WSMCs under seismic loading are proposed and evaluated through FE analysis. The first involves the attachment of a steel plate to the beam web and

column flange in the anticipated plastic hinge region. This "web reinforcement" (shown in Fig. 6a) is designed to reduce the slenderness of the beam web in the region of anticipated buckling and provide greater resistance to flexural buckling and twisting. By combining the web reinforcement with the HBS, plastic hinging of the beam still takes place away from the welded joint, however strength degradation is delayed and the rate of strength loss is reduced. The combination of these two features (HBS and web reinforcement) creates a connection that is resilient to both local buckling and weld fatigue failures. This connection is referred to as HBS-WR in the forthcoming discussion.

As an alternative to web reinforcement, reduction of the material strength of the beam web in the plastic hinge is proposed. This reduction of the material strength simply involves extending the HBS to the beam web as shown in Fig. 6b. As a consequence, flexural (and shear) stresses are reduced in the beam web without making any adjustments to the geometry. The heat treatment does not reduce the plastic modulus of A992 steel (note the downward shift of the stress-strain curve shown in Fig. 2b¹), therefore, with reduced bending stresses acting on the beam web in the plastic hinge, and no deterioration of the material plastic modulus, less buckling damage and strength degradation is likely as a result.

By extending the heat treatment to the web of the beam, the cross section of the beam in the plastic hinge is made homogeneous with respect to material yield strength. Based on Eq. (1) and Fig. 1c and d, with all else being equal, a reduction of material yield strength as shown in Fig. 2b may significantly improve plastic rotation capacity. The proposed connection involving the extension of the HBS to the beam web is referred to as HBS-W in the forthcoming discussion.

It is important to note that the primary goal of the proposed modifications is to delay the onset and slow the rate of connection strength degradation due to local beam buckling and not necessarily to increase the moment capacity of the beam. While strength increase may accompany the primary objectives, a significant increase in connection strength is generally unnecessary as the design of moment resisting frames tends to be governed by the serviceability and not the strength limit state [22]. In addition, significant strength increase may require additional strengthening of the column in order to avoid violating strong-column-weak-beam (SCWB) criteria and excessive panel zone shear distortions.

3.1. Finite element modeling of enhanced connections

Three dimensional (3D) nonlinear finite element models were developed for the proposed connections using the commercial finite element analysis software ANSYS Mechanical ADPL [23]. Geometric and material nonlinearities were incorporated in the finite element models. An example of the finite element mesh and boundary conditions is shown in Fig. 7a and b. Displacement boundary conditions were applied so as to simulate typical experiment support conditions [20], therefore hinge supports were applied to the columns ends while roller supports were applied to the beam flanges close to the loading point (to provide lateral bracing). Displacements were applied to the beam tip in accordance with the standard ANSI/AISC 341–10 [3] loading protocol for SMF connections.

The beam, column, web reinforcement and continuity plates were modeled with 8 noded solid hexahedral elements (SOLID185) with selective reduced integration scheme. Welding attachment of the web reinforcement plate to the beam web and column flange was simulated by prescribing multi-point displacement constraints between the nodes of the web reinforcement plate, column flange and beam web as shown in Fig. 7b. This method has been used in previous studies [4] to simulate reinforcing fillet welds between the beam web and shear tab in WUF-W connections. The weld pattern shown in Fig. 7b is intended to simulate

attachment of the web reinforcement plate through slot welds on the interior portion of the plate and fillet welds around the edges. The thickness of the web reinforcement plate and its weld attachment to the beam web was decided through trial and error. It was found that for the W30 \times 148 beam section studied, a plate thickness matching or slightly greater (3.2 mm or 1/8 in.) than the beam web thickness produced optimal results. The web reinforcement plate is intended to be shop welded to the beam web and then field welded to the shear tab.

Finite element models accounted for material nonlinearity through rate-independent metal plasticity theory based on additive strain decomposition, the Von Mises yield criterion, associated flow rule and Chaboche non-linear kinematic hardening rule [24]. The distinctive feature of the Chaboche model is the superposition of non-linear kinematic hardening rules according to Eqs. (6) and (7). This allows for accurate simulation of hysteric loop shape over a wide strain range. A brief description of the Chaboche [24] model is given below.

Additive decomposition of each strain increment into elastic and plastic parts is considered:

$$d\varepsilon = d\varepsilon^e + d\varepsilon^p \tag{3}$$

The elastic strain increment $(d\varepsilon^e)$ is calculated by the generalized Hooke's law. The Von-Mises yield criterion is expressed as:

$$f(\underline{\sigma} - \underline{\alpha}) = \left[\frac{3}{2} (\underline{s} - \underline{a}) \cdot (\underline{s} - \underline{a}) \right]^{\frac{1}{2}} = \sigma_0 \tag{4}$$

where $\underline{\sigma}$ is the stress tensor, $\underline{\alpha}$ is the current center of the yield surface in the total stress space, \underline{s} is the deviatoric stress tensor, \underline{a} is the current yield surface center in the deviatoric space, and σ_0 is the radius of the yield surface.

The plastic strain increment $(d\varepsilon^p)$ is calculated using the associated flow rule:

$$\frac{d\underline{\varepsilon}^{p} = d\lambda \frac{\partial f}{\partial \underline{\sigma}} = \frac{3}{2} dp\underline{s} - \underline{a}}{\sigma_{0}}$$
(5)

Where the $d\lambda$ is the plastic strain multiplier and dp is the scalar plastic strain increment.

The superimposed kinematic hardening rule is given by:

$$d\underline{a} = \sum_{i=1}^{n} d\underline{a} \tag{6}$$

$$d\underline{a}_{i} = \frac{2}{3}C_{i}d\underline{\varepsilon}^{p} - \gamma_{i}\underline{a}_{i}dp \tag{7}$$

Each of the superposed kinematic hardening rules has a strain hardening term (1st term in Eq. (7)) and a dynamic recovery term (2nd term in Eq. (7)). C and γ are material parameters obtained from fitting a stable single amplitude stress-strain curve from a uniaxial cyclic material test as shown in Fig. 7c for A992 steel.

Geometric nonlinearities were accounted for via a large deformation formulation. During the development of these finite element models it was found that with the cyclic displacement loading history applied to the beam-column connections, local buckling of the beam is predicted without the introduction of any eccentricities either from initial geometric imperfections or small lateral loads. This observation has also been made by Myers [25]. Despite the symmetry of the mesh, boundary conditions and applied loads, small eccentricities accumulate during cyclic loading. These eccentricities provide perturbation for local buckling simulation and in some cases produces results of reasonable accuracy. However, the same is not true of monotonic simulations; in fact, a monotonic FE simulation of a beam to column moment connection with symmetric geometry, boundary conditions and loads will highly

 $^{^{1}\,}$ In fact the work hardening rate of A992 steel increases as a consequence of heat treatment. The yield strength is reduced by 38%, but the tensile strength is reduced by 25%.

over predict the connection capacity and fail to accurately predict local buckling.

In general, accurate numerical prediction of experimentally observed local buckling is challenging partly because the actual geometric imperfections of the structure can be quite complex and difficult to measure and model. Cyclic simulations in which buckling is perturb by accumulated eccentricities can be viewed as an upper bound solution and may in some instances make un-conservative predictions. Therefore, in this study initial geometric imperfections were imposed by first conducting an eigenvalue analysis of the perfect structure and then prescribing a scaled value of the first eigenmode displacement field as the initial configuration of the structure. The scaling was chosen to represent realistic values of W-shape "out of squareness" based on ASTM A6 [26] tolerances. Similar approaches have been used in other studies [27,28].

To validate the FE model, the moment-plastic rotation response of HBS 5 is simulated and compared to the experiment in Fig. 7d. In addition, the simulation of the cross-section displacements with progressive local web and flange buckling of HBS 5 at a section 406 mm from the column face is compared to the experimentally measured displacements in Fig. 5. The calculated connection plastic rotation during each loading cycle as well as the peak moments shows good comparison with the experimental responses (Fig. 7d). In addition, the cross-section displacement predictions (Fig. 5) show very good correlation with the measured values and appear to accurately capture the initiation and progression of local buckling of HBS 5.

3.2. Finite element analysis results and discussion

In order to quantify and analyze the effectiveness of the proposed methods, response parameters used by Uang and Fan [10] namely, plastic rotation capacity (θ_{pc}) and strength degradation rate (SDR) (which were introduced earlier) are adopted in this study with one minor change. The SDR is redefined as the ratio of connection resistance (bending moment) at the plastic rotation corresponding to the maximum strength θ_{pM_n} to the connection resistance (bending moment) at 0.01 rad plastic rotation greater than θ_{pM_n} , i.e. $\theta_{pM_n} + 0.01$.

$$SDR = \frac{M_{@\theta_P M_n}}{M_{@\theta_P M_n + 0.01}} \tag{8}$$

This definition attempts to quantify the rate of strength loss immediately following the initiation of strength degradation regardless of the plastic rotation at which the onset of strengthen degradation occurs. This redefinition of the SDR was deemed appropriate for this study since in some cases connections may not experience strength loss between 0.02 and 0.03 rad plastic rotation as was assumed by Uang and Fan [10,11]. Response parameters were computed for both positive and negative bending and the average values are reported.

Proposed connections HBS-WR and HBS-W were subjected to cyclic loading prescribed according to the ANSI/AISC 341-10 [3] loading protocol for SMF connections. In the simulations the applied beam tip displacements were increased in accordance with the loading protocol until the connection strength had degraded below 80% of its maximum value. The moment-plastic rotation envelops for the proposed connections are compared to the earlier presented HBS 5 and HBS 7 connection experimental and simulation responses in Fig. 8. It is noted that while the geometry of HBS 5 and HBS 7 was identical, their material yield strengths varied [20]. This accounts for the noticeable variation in their moment responses. The moment-plastic rotation envelops in Fig. 8 were used to determine the plastic rotation capacities and strength degradations rates tabulated in Table 1. In addition, the accumulated equivalent plastic strain contour plots at 5% story drift for HBS, HBS-W and HBS-WR simulations are presented in Fig. 9. Note that in the simulations the beam and column sections, dimensions, boundary conditions and loading history for HBS-WR and HBS-W connections are identical to

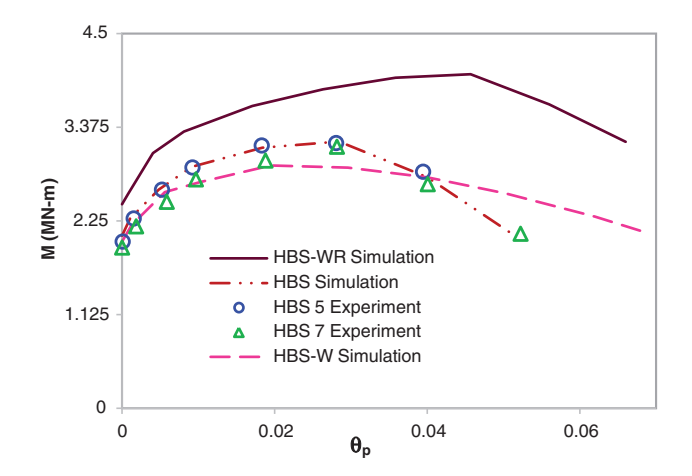


Fig. 8. Moment-plastic rotation backbone curves for HBS connections (experiment and simulation).

that used for the HBS connection. Analysis of Table 1 and Figs. 8 and 9 have led to the observations discussed in the following.

The addition of the web reinforcement plate increases post yield connection stiffness and strength (see Fig. 8). It also delays the onset of buckling, increases the plastic rotation capacity by 50%, and gives a mild improvement in the strength degradation rate (see Table 1). As a result, energy dissipation is improved significantly and buckling damages are also reduced (compare Fig. 9a and b with e and f).

As an alternative, extending heat-treatment to the beam web (HBS-W) reduces connection strength (Fig. 8). Though it does not delay the onset of strength loss, it significantly reduces the rate of degradation (Fig. 8) and the associated local buckling damage in the plastic hinge (compare Fig. 9a and b with c and d). As a result, extending heat-treatment to the beam web improves the plastic rotation capacity by 40% and also contributes to a significant improvement in the SDR (see Table 1).

In addition to improving buckling resilience, the proposed strategies are also fatigue resilient as in both cases most of the yielding and damage takes place away from the welded joint (see Fig. 9). Although being more involved from a fabrication standpoint, beam web reinforcement (HBS-WR) does seem to provide greater improvements in seismic performance. Based on these results, full scale testing was conducted to validate the web reinforcement technique as described in the following.

4. Experimental validation

One large scale exterior moment frame sub-assemblage specimen (HBS 8) was tested to evaluate the performance enhancement provided by the web reinforcement. The test setup and details of the test specimen are shown in Fig. 10. The beam and column section sizes, lengths, and support conditions were chosen to be identical to those of HBS 5 and HBS 7. In addition, the welding details for the attachment of the beam flange and beam web to the column flange (shown in Fig. 10b) remained identical to those of HBS 5 and 7. This allowed for direct comparisons to be made between the performance of otherwise identical connections with and without web reinforcement.

Table 1Plastic rotation capacity and strength degradation ratios of HBS WSMCs.

Connection ^a	θ_{pc} (radians)	SDR
HBS 5	0.039	0.91
HBS 7	0.041	0.88
HBS-WR	0.061	0.92
HBS-W	0.056	0.99

 $^{^{}a}\,$ All connections have the same beam (W30 \times 148) and column (W14 \times 148) cross-sections.

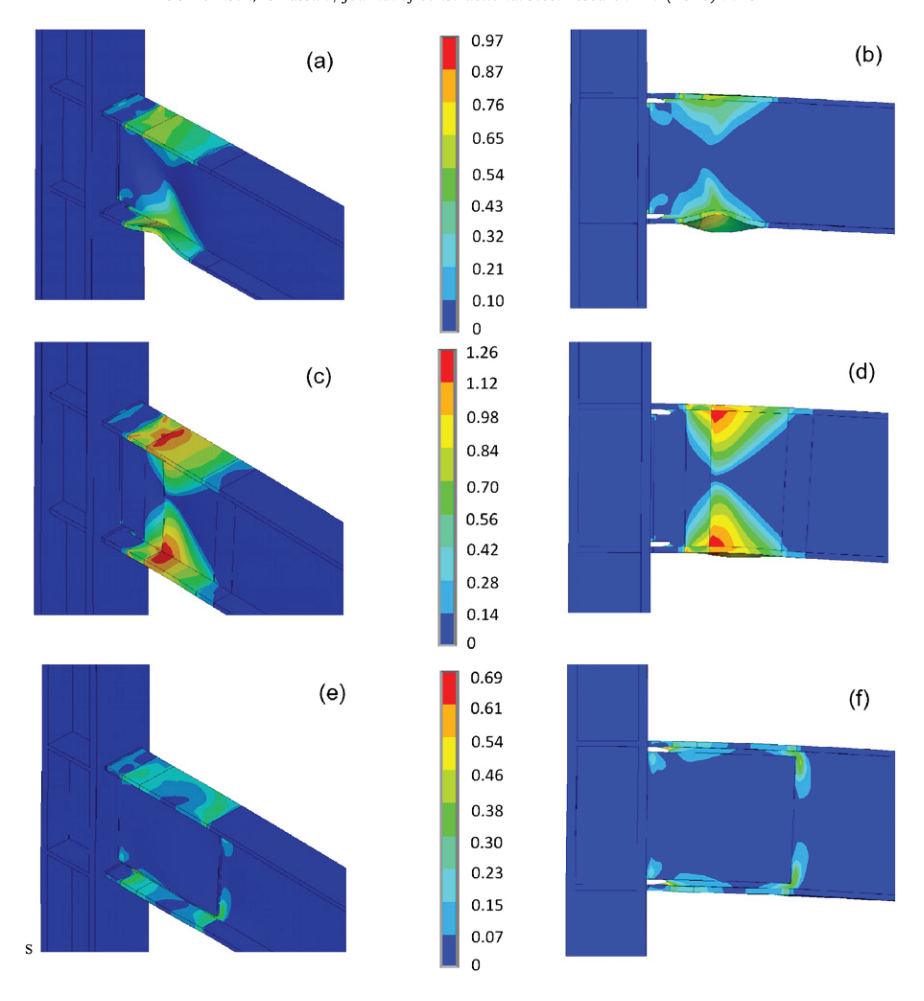


Fig. 9. Equivalent Plastic strain contours at 5% story drift for moment connecitons (a) HBS (isometric) (b) HBS (elevation) (c) HBS-W (isometric) (d) HBS-W (elevation) (e) HBS-WR (isometric) (f) HBS-WR (elevation).

The web reinforcement plate was fabricated in the shop with horizontal and vertical slots as shown in Fig. 10b and d. Shop welding of the web reinforcement plate to the beam web was accomplished using gas shielded metal arc welding (GMAW) with E71T-1C-H8 electrodes which are specified to meet the requirements of AWS D1.8. Fillet welds were used to connect the perimeter of web reinforcement plate to the beam web and were also placed in the vertical and horizontal slots to provide added reinforcement to the beam web. This design (length and pattern of welds) was determined using the FE modeling presented earlier (see Section 3).

Upon completion of beam fabrication, heat treatment was performed using electrical resistance ceramic mat heating pads as shown in Fig. 11a. Heating pads were sized according to the required dimensions of the HBS and were installed on the inner and outer surface of the beam flanges. The heating pads were connected to a power supply and type K thermocouples were used to monitor temperatures and provide continuous feed back to the power supply. Three (3) layers of 50 mm (2 in.) high density ceramic fiber insulation blankets were wrapped around the beam flanges as shown in Fig. 11b to provide well controlled heating and cooling. More details about the heat treatment setup and procedure are provided in [20,29].

Connection welding was performed outdoors with the column oriented vertically (similar to actual field conditions) by a welder qualified in accordance with the requirements of AWS D1.1-10 and AWS D1.8-09. Welding was accomplished with self-shielded flux cored arc welding (FCAW) process. E70-T6 electrodes were used for beam flange complete joint penetration (CJP) welds which were made in the down hand position, while E71-T8 electrodes were used for the beam web CJP weld and

reinforcing fillet welds which were made in the vertical and overhead positions respectively. Both of these electrodes were specified by the manufacturer to deposit metal with a minimum Charpy V-notch toughness of $27 \,\mathrm{J}$ ($20 \,\mathrm{ft}$ -lbs.) at $-28 \,^\circ\mathrm{C}$ ($-20 \,^\circ\mathrm{F}$). The bottom flange backing bar was removed and a reinforcing weld was placed at the root of the grove weld. The top flange backing bar was left in place, however a fillet weld was provided between the backing bar and the column flange. Weld tabs from the top and bottom beam flange CJP welds were removed by carbon air arc gouging. After the beam to column CJP welds were completed, a CJP weld was installed between the shear tab and the web reinforcement plate as shown in Fig. 10b. Finally, all CJP welds were ultrasonically (UT) tested by a certified welding inspector (CWI) in conformance with AWS D1.1-10 and AWS D1.8-09. More details on the welding procedures, specifications and parameters are provided in [29].

Each specimen was equipped with strain gauges along the beam flanges to monitor longitudinal flange strains at various locations including the weld toe and HBS region. String and linear potentiometers were used to monitor displacements and rotations in the beam, column, and panel zone. A calibrated load cell in the hydraulic actuator provided readings of force response during the experiment. The specimen was also painted with hydrated lime prior to testing to visually indicate regions of yielding.

The Optotrak Certus HD three-dimensional (3D) position system was used to capture the positions of markers placed along the beam flanges and web (Fig. 3). Position time history data obtained from this system was post processed to calculate displacements and strains in areas of interest.

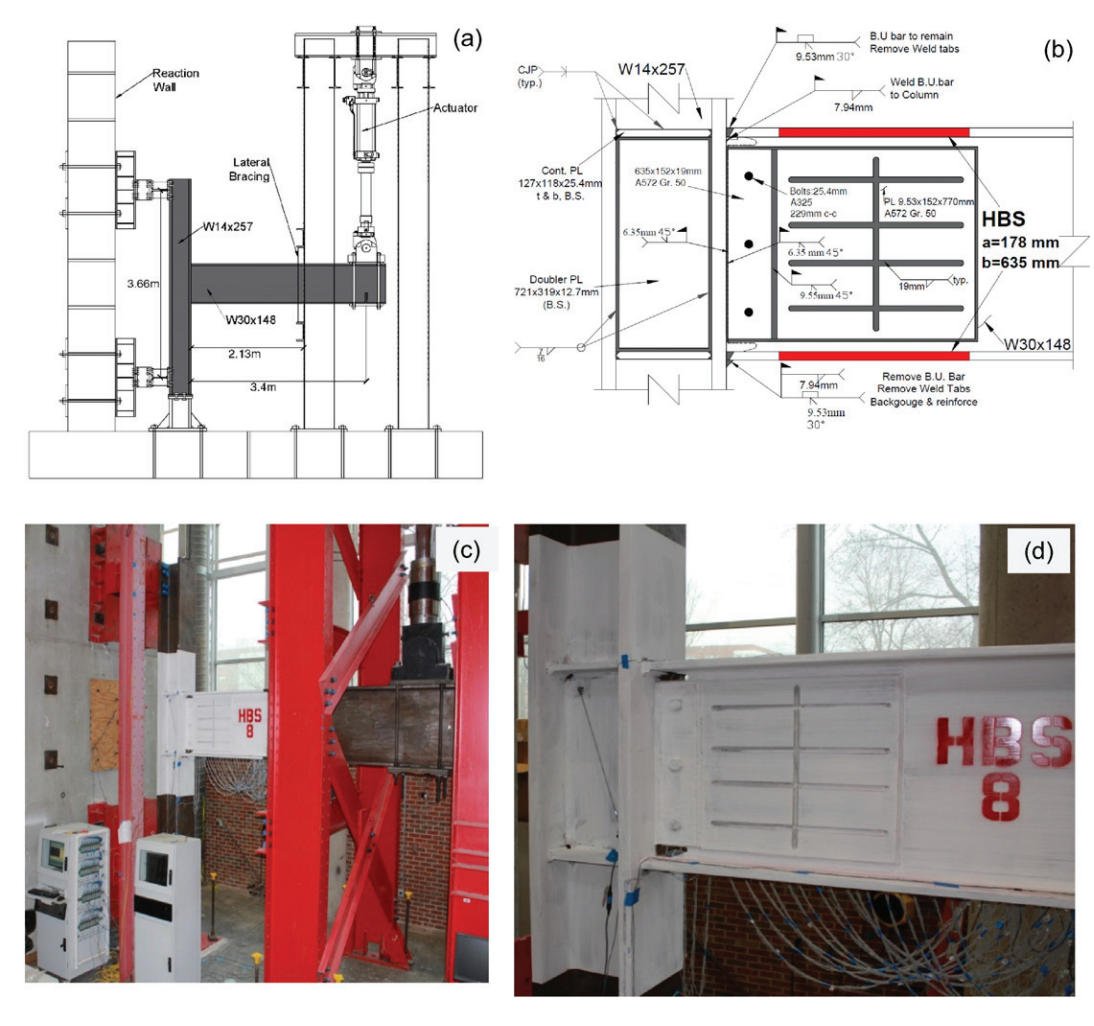


Fig. 10. HBS 8 test setup and connection details a) sketch of the test setup, b) sketch of the connection details, c) photograph showing test setup and, d) photograph of HBS 8 connection prior to testing.

5. Test results

5.1. Global response of HBS 8

Testing was conducted at the North Carolina State University Constructed Facilities Laboratory (CFL). Loads were applied at the beam tip in accordance with the 2010 ANSI/AISC 341-10 [3] loading protocol consisting of quasi-static increasing amplitude displacement cycles. Fig. 12a shows the moment-rotation response of HBS 8. This global response shows wide and stable hysteresis loops. HBS 8 met the 2010 AISC Seismic Provisions (ANSI/AISC 341-10) SMF qualifying 4% interstory drift angle without strength loss. Slight strength degradation due to a fracture

sustained in the fillet weld of the vertical slot in the center of the web reinforcement plate, was observed during the 1st cycle of loading at 5% story drift. Photographs of this fracture are shown in Fig. 16 and will be discussed more later. Loading of HBS 8 was terminated after completing 1 cycle at 5% story drift as a result of this failure.

5.2. Comparative analysis of HBS 8

5.2.1. Global response

The peak moment-plastic rotation response of HBS 8 is compared to those of HBS 5 and HBS 7 in Fig. 14. As anticipated from pretest analysis, HBS 8 displays increased strength and stiffness compared to HBS 5 and





Fig. 11. Heat-treatment setup (a) photograph showing electric surface heating pads during installation on a beam flange [20], (b) photograph showing insulation of beam flange for well controlled heating and cooling [20]

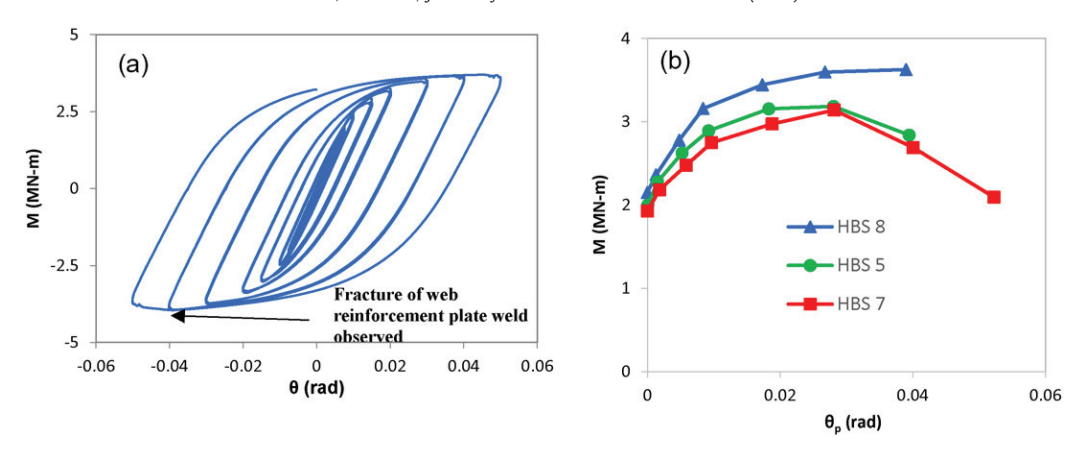


Fig. 12. (a) Moment-rotation response of HBS 8 (b) Moment-plastic rotation backbone curves for HBS 5, HBS 7 and HBS 8.

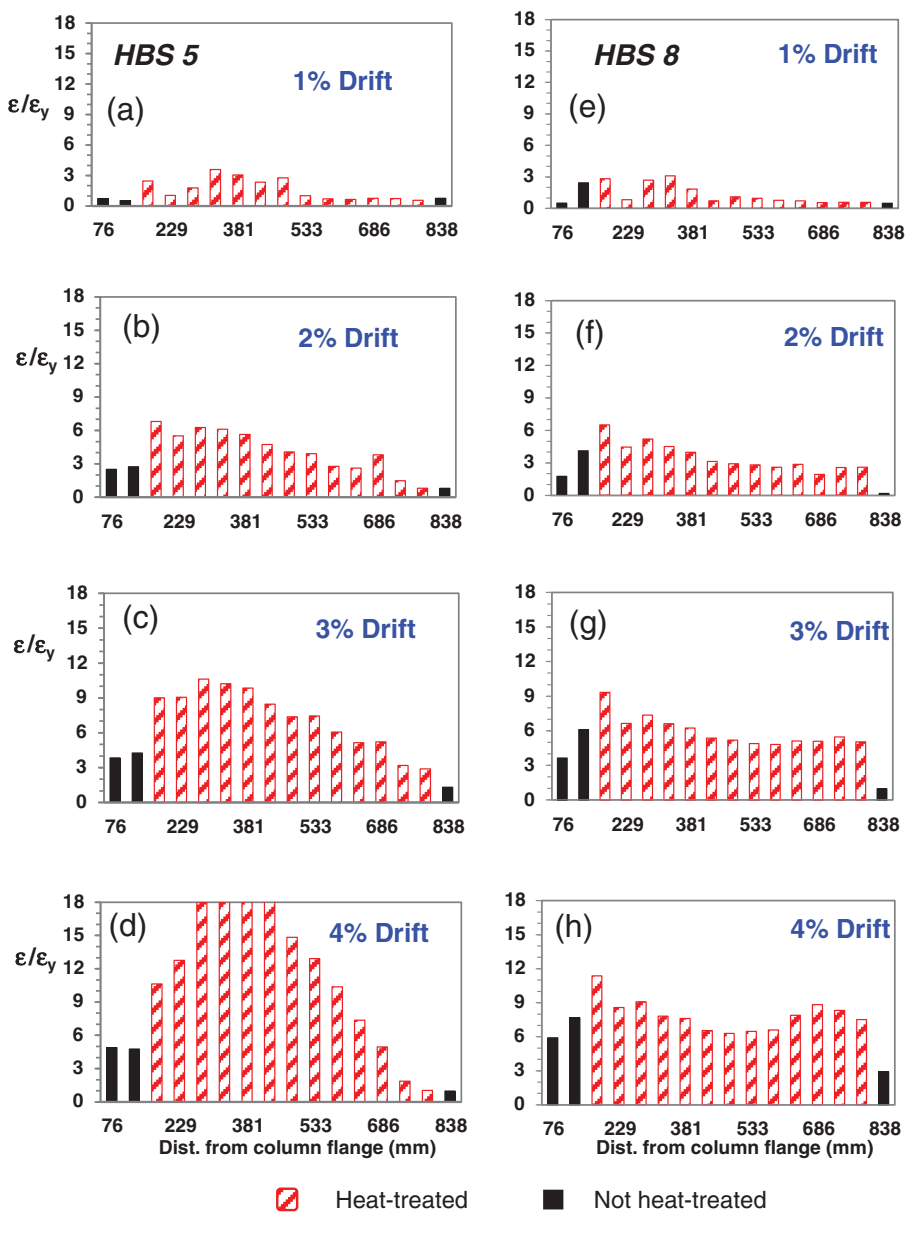


Fig. 13. Recorded longitudinal strains along the center of the beam top flange (a-d) HBS 5 and (e-h) HBS 8.

HBS 7. The onset of strength degradation was also delayed in HBS 8 which validates the concept of improving buckling resistance of wide flange beam to column HBS moment connections through web reinforcement.

5.2.2. Plastic hinge formation

Fig. 13 compares the progression of flexural strains along the beam top flange for HBS 5 and HBS 8. These bar graphs show the distribution of longitudinal tensile strains (normalized by the yield strain) along the centerline of the beam flange at various stages of the loading history.

Bars highlighted in red represent the strains in the heat-treated (weak-ened) regions. Strains were calculated by post processing data obtained from the Optotrak Certus HD (3D) position system sensors placed along the beam top flange. Comparison of the strain responses show that the combination of the web reinforcement plate and HBS results in more widely (less concentrated) distributed beam flange flexural strains over the plastic hinge region. As a result, at comparable drift angles, strain demands are lowered in the heat treated region in HBS 8. This effect leads to a favorable condition both in terms of fatigue resistance and delay of beam flange local buckling.

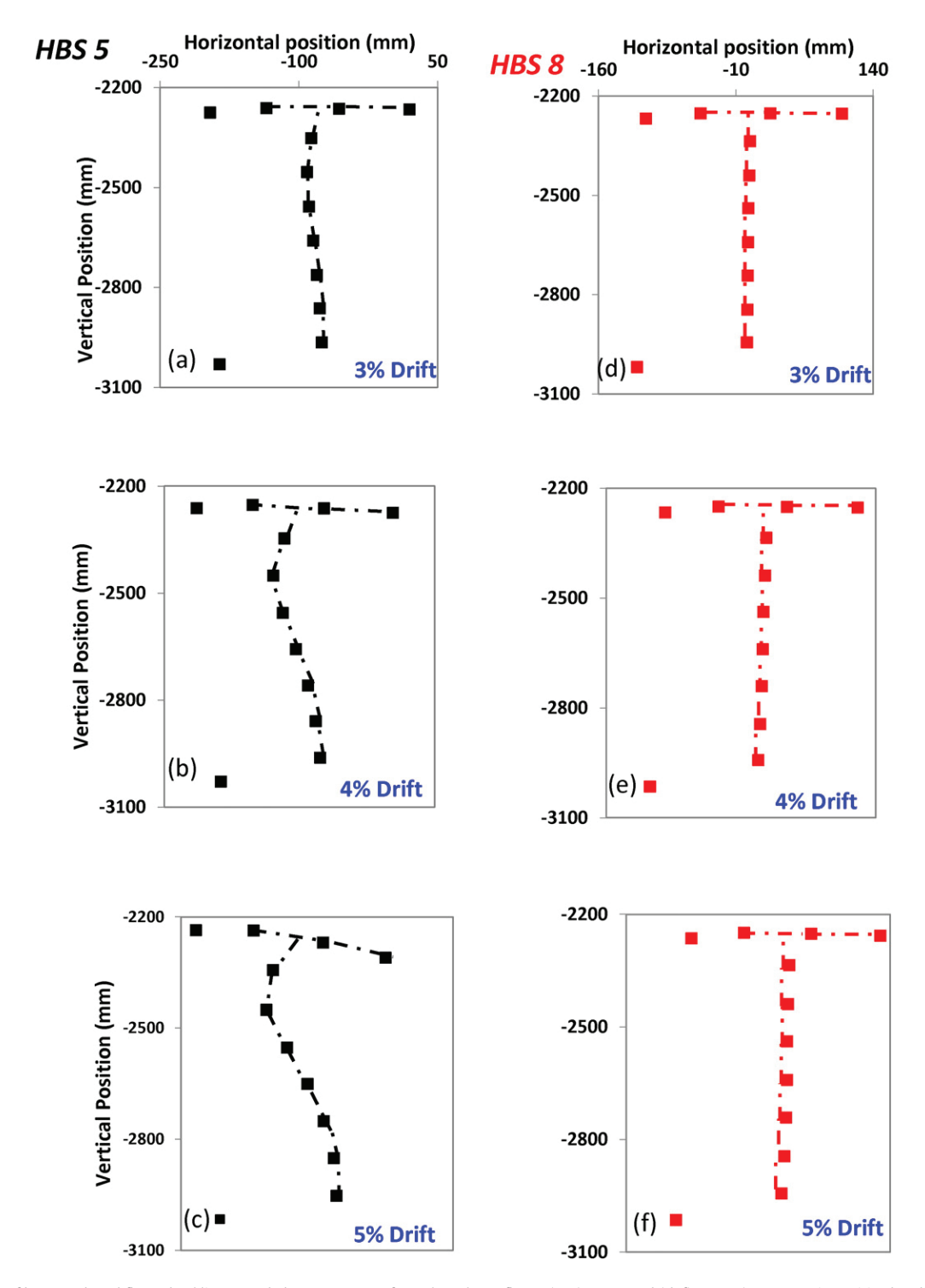


Fig. 14. Progression of beam web and flange buckling recorded 406 mm away from the column flange (a–c) HBS 5 and (d–f) HBS 8 (Beams are in positive bending i.e. top flange in compression).

5.2.3. Local buckling

Fig. 14 compares planar displacements of the beam cross-section located 406 mm away from the column flange of HBS 5 and HBS 8 at 3%, 4% and 5% interstory drift. Dotted lines have been traced between data points to make evident the progressive buckling of the beam. Fig. 15 compares photographs of HBS 5 and HBS 8 at corresponding stages of the loading history. These two figures provide validation of the web reinforcement plate technique in significantly reducing FLB, WLB and LTB for HBS beam to column moment connections. Note that even though no reinforcement of the flanges was provided, flange local buckling is significantly reduced by the presence of the web reinforcement plate (compare Fig. 15c and f). This supports the findings of Uang and Fan [10,11] and Okazaki et al. [13] who both demonstrated the interaction between non dimensional web and flange slenderness parameters through nonlinear regression analysis. Evidence from the experimental results presented in this article suggests that WLB and FLB are at least weakly coupled. Reduced flexural strains along the beam flanges as demonstrated in Fig. 13 may have been a contributing factor to the reduced local flange buckling observed in HBS 8.

5.2.4. HBS 8 Web reinforcement plate fillet weld failure

As previously stated, loading of HBS 8 was terminated after one complete loading cycle at 5% story drift due to a crack in the bottom of the fillet weld in the vertical slot of the web reinforcement plate.

Photographs of the failure location and rupture are shown in Fig. 16a and b respectively. The crack which measured 127 mm (5 in.) in length propagated through the beam web and extended vertically as shown in Fig. 16b, resulting in strength loss as shown in Fig. 12a. This failure underscores the well-established understanding that fillet welds are less ductile when loaded perpendicular to their longitudinal axes. In addition, the "v-shaped" topography of the fillet welds in the web reinforcement plate slots (Fig. 16b and c) create an unfavorable stress concentration which may have also contributed to this failure.

6. Future work on proposed techniques

Due to the limitation of resources, this study was conducted on a rolled wide flange section with relatively compact web and flange elements. As demonstrated in the above review of the literature, WSMCs constructed with rolled wide flange beams do suffer from severe strength degradation due to buckling. However, many of these rolled wide flange sections satisfy the requirements for highly ductile members in the 2010 ANSI/AISC seismic provisions [3] and as a result are able to meet the 0.03 rad plastic rotation capacity required for use in SMFs (see Fig. 1d). Therefore, the strategies outlined in this article are anticipated to add greater value in enhancing the buckling resistance of built-up I-shaped beams whose web and flange elements don't satisfy width-to-thickness ratios of highly ductile members according to the

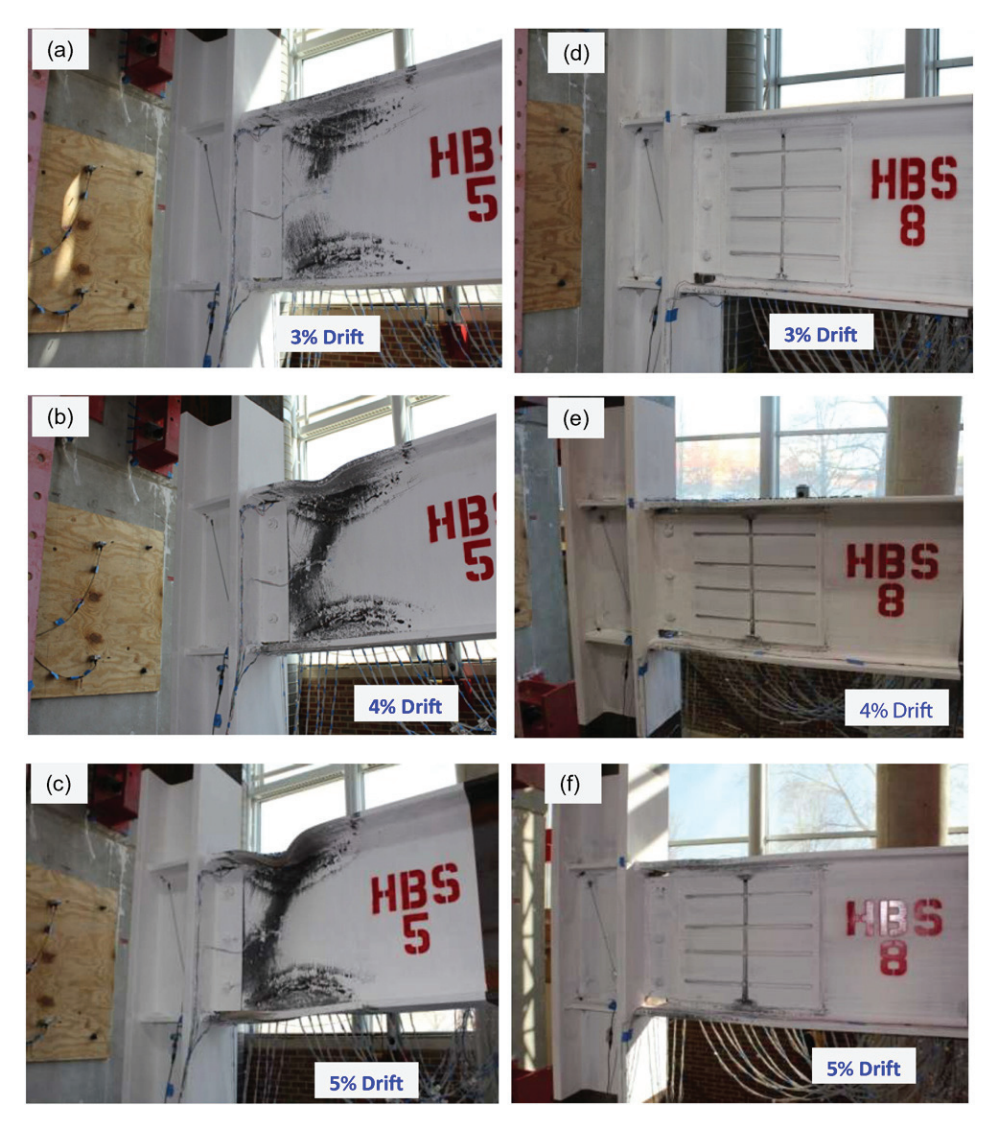


Fig. 15. Photographs comparing the yielding, plastic hinging and local buckling at various stages of the loading history for (a-c) HBS 5 and (d-f) HBS8.

2010 ANSI/AISC seismic provisions [3], thus limiting their applicability to intermediate or ordinary moment frames. For example, Figs. 1d, e and 2b show that with the reduction of yield strength by the heat treatment (Fig. 2b), the plastic rotation capacity of a grade 50 steel beam that does not satisfy width-to-thickness ratios to be considered highly ductile [3] (i.e. a beam with h/t_w ratio lying above the horizontal dashed line and/or a $b_f/2t_f$ ratio lying to the right of the vertical dashed line shown in Fig. 1d) can be significantly improved as shown in Fig. 1e. FE analysis of HBS-W supports this prediction. The web reinforcement plate also provided significant improvement to plastic rotation capacity and was experimentally validated. In addition, both of the proposed techniques have the potential to be used as retrofit techniques for seismic upgrades.

The research conducted in this study falls far short of that needed for development of design details and equations, therefore, further studies are necessary to continue to develop and improve these methods. Future studies on the web reinforcement technique should incorporate more detailed FE analysis to optimize the reinforcement plate weld attachment design so as to minimize stress and strain concentrations, welding induced distortions and cost. It is recommended that vertical slots with fillet welds be avoided based on the results of the current study. In addition, experimental validation is required for the HBS-W technique. It is recommended that future numerical and experimental studies should include application of these techniques to built-up I-shaped beams whose web and flange elements may only satisfy width to thickness ratios to be considered moderately ductile according to the 2010 ANSI/AISC seismic provisions [3].

Another attractive application of these techniques (particularly the web reinforcement technique) may be their use at the column base plastic hinge location in moment frames which employ deep columns (W27 and deeper sections). These deep members have reduced torsional properties and more slender web and flange elements when compared to the W14 and shallower sections traditionally used for columns in gravity frames. In addition, unlike beams, these members carry compressive axial loads (from gravity forces) and are expected to sustain large plastic rotations during the formation of a beam sway mechanism in a severe earthquake. Recent experimental [30] and analytical research [31] on the behavior of deep columns (constructed

from rolled wide flange sections) in moment frames subjected to combined lateral and axial loads have shown them to be susceptible to severe strength degradation at interstory drift levels below the required 4%. Web slenderness was found to play a significant role in this strength degradation mechanism [31] and as such, it is anticipated that the techniques outlined in this study may provide a viable solution to this problem.

7. Conclusion

Strength degradation initiated by local buckling damages in WSMC's has been studied experimentally and through FE analysis. This strength degradation is observed to be initiated by buckling of the beam web which is followed by buckling of the beam flange and lateral torsional buckling in the plastic hinge. It is observed that once this strength degradation initiates it propagates quickly with continued incremental cycles. By 4% interstory drift test data show that local beam web and flange buckling damages in the plastic hinge region become large. To counter this, two techniques for improving the seismic performance of HBS WSMCs have been proposed and studied through finite element analysis. One technique involves welding a reinforcement plate to beam web and column flange in the plastic hinge region, while the other technique involves extending the HBS to the beam web. FE studies show both techniques to be fatigue resilient (i.e. plastic hinge forms away from welded joint) and to reduce local buckling damage and associated strength degradation.

The web reinforcement technique was validated through full scale simulated seismic testing. Test results show the web reinforcement to be effective in improving stiffness, reducing buckling damages and delaying the onset of strength degradation of HBS WSMCs. Results show that these benefits are obtained without changing the plastic hinge location. In fact, it was observed that the addition of the web reinforcement plate results in more widely distributed (less concentrated) flexural strains in the plastic hinge. However, test results also show that careful detailing of the welding attachment of the reinforcement plate to the beam web is necessary to circumvent unwanted failures to these welds.

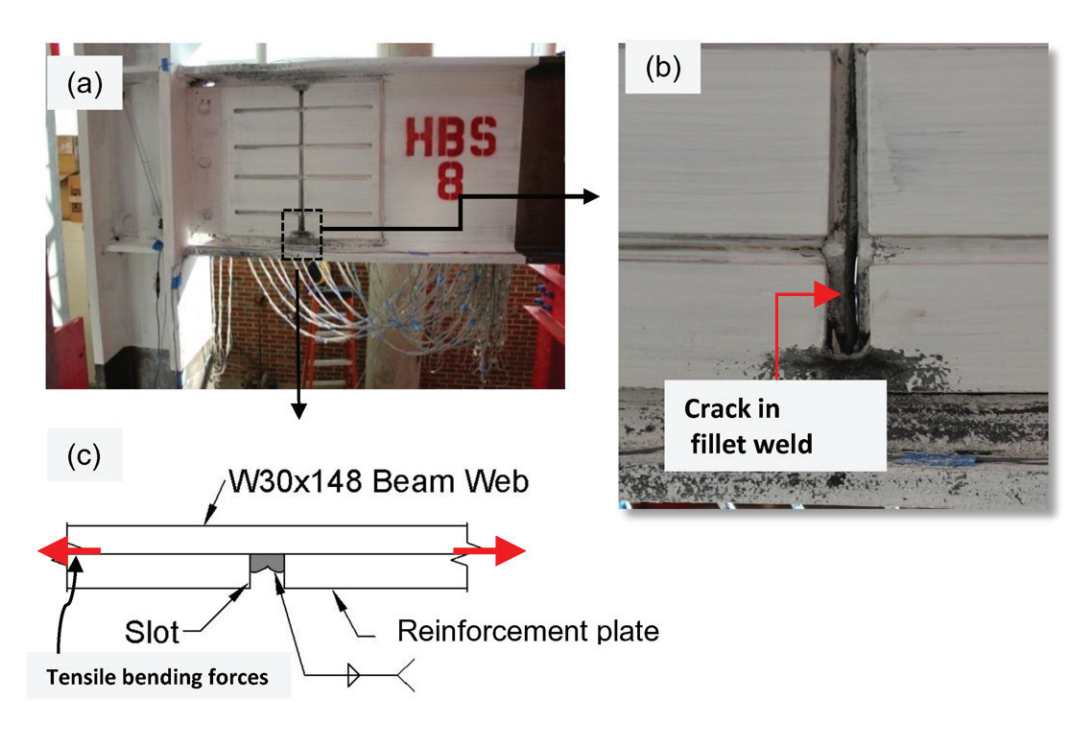


Fig. 16. (a) Post-test photograph showing fracture of web reinforcement plate fillet weld and beam web (b) enlarged photograph at the fracture location (c) Sketch of web reinforcement slot fillet weld detail.

Areas for application of these techniques such as seismic upgrades or new construction of moment frames involving non-compact beams, and the reinforcement of column bases constructed from deep wide flange sections have been identified. Suffice it to say that future analytical and experimental studies are needed to further develop and eventually implement these techniques in the field. In this regard, the experimental and analytical findings of the current study should provide a valuable starting point for such efforts.

Acknowledgment

Funding for this research was provided by the National Science Foundation under the Network for Earthquake Engineering Simulation (NSF Grant no. 0936547). However, any opinions presented in the paper are solely those of the authors. The authors greatly acknowledge the efforts and assistance provided by the staff of Furmanite Inc., Steel Fab Inc., Flores Welding Inc. and the Constructed Facilities Laboratory (CFL) at NCSU. In addition, the efforts of Shahriar Quayyum and Doug Schweizer in the early stages of this research study are acknowledged.

References

- FEMA-355D, State of the Art Report on Connection Performance, Prepared by the SAC Joint Venture for the Federal Emergency Management Agency, Washington, DC, 2000.
- [2] AISC/ANSI 358-10, Prequalified Connections for Special and Intermediate Steel Moment Frames for Seismic Applications, Chicago, 2010.
- [3] AISC/ANSI 341-10, Seismic Provisions for Structural Steel Buildings, Chicago, 2010.
- [4] J.M. Ricles, C. Mao, L.W. Lu, J.W. Fisher, Development and Evaluation of Improved Details for Ductile Welded Unreinforced Flange Connections, SAC Joint Venture: Report SAC BD-00/24, 2000.
- [5] S.L. Jones, G.T. Fry, M.D. Engelhardt, Experimental evaluation of cyclically loaded reduced beam section moment connections, J. Struct, Eng. 128 (2002) 441–451.
- [6] E.A. Sumner, T.M. Murray, Behavior of extended end-plate moment connections subject to cyclic loading, J. Struct. Eng. 128 (4) (2002) 501–508.
- [7] S.P. Schneider, I. Teeraprbwong, Inelastic behavior of bolted flange plate connections, J. Struct. Eng. 128 (2002) 492–500.
- [8] S.M. Adan, W. Gibb, Experimental evaluation of Kaiser bolted bracket steel momentresisting connections, Eng. J. (2009) 181–195.
- [9] Q. Yu, S. Yu, C. Gilton, C.M. Uang, Cyclic response of RBS moment connections: loading sequence and lateral bracing effects, SAC Joint Venture: Report SAC BD-00/22, 2000.
- [10] C.M. Uang, C.C. Fan, Cyclic instability of steel moment connections with reduced beam section, SAC Joint Venture: Report SAC BD-99/19, 1999.
- [11] C. Uang, C. Fan, Cyclic stability criteria for steel moment connections with reduced beam section, J. Struct. Eng. 127 (9) (2001) 1021–1027.

- [12] AISC/ANSI 358-02, Seismic Provisions for Structural Steel Buildings, Chicago, 2002.
- 13] T. Okazaki, D. Liu, M. Nakashima, M.D. Engelhardt, Stability requirements for beams in seismic steel moment frames, J. Struct. Eng. 132 (9) (2006) 1334–1342.
- [14] AISC/ANSI 358-05, Seismic Provisions for Structural Steel Buildings, Chicago, 2005.
- [15] T. Kim, A.S. Whittaker, V.V. Bertero, A.S.J. Gilani, S.M. Takhirov, Steel moment resisting connections reinforced with cover and flange plates, SAC Joint Venture: Report SAC BD-00/27, 2000.
- [16] W. Wang, Y. Zhang, Y. Chen, Z. Lu, Enhancement of ductility of steel moment connections with noncompact beam web, J. Constr. Steel Res. 81 (2013) 114–123.
- [17] F. Li, I. Kanao, J. Li, K. Marisako, Local buckling of RBS beams subjected to cyclic loading, J. Struct. Eng. 135 (12) (2009) 1491–1498.
 [18] S.H. Chao, K. Khandelwal, S. El-Tawil, Ductile web fracture initiation in steel shear
- [18] S.H. Chao, K. Khandelwal, S. El-Tawil, Ductile web fracture initiation in steel shear links, J. Struct. Eng. 132 (8) (2006) 1192–1200.
- [19] T. Okazaki, M.D. Engelhardt, M. Nakashima, K. Suita, Experimental performance of link-to-column connections in eccentrically braced frames, J. Struct. Eng. 132 (8) (2006) 1201–1211.
- [20] M. Morrison, D. Schweizer, T. Hassan, An innovative seismic performance enhancement technique for steel building moment resisting connections, J. Constr. Steel Res. 109 (2015) 34–46.
- [21] M.L. Morrison, D.Q. Schweizer, T. Hassan, Seismic enhancement of welded unreinforced flange-bolted web steel moment connections, J. Struct. Eng. (2016), 04016102.
- [22] SEAOC, 2012 IBC Structural/Seismic Design Manual, Example for Steel-Framed Buildings, vol. 4, Structural Engineers Association of California, Sacramento, CA, 2013.
- [23] ANSYS® Academic Research, Release 14.5, Help System, Structural Analysis Guide, ANSYS, Inc (2012).
- [24] J.L. Chaboche, Time-independent constitutive theories for cyclic plasticity, Int. J. Plast. 2 (2) (1986) 149–188.
- [25] A. Myers, Testing and Probabilistic Simulation of Ductile Fracture Initiation in Structural Steel Components and Weldments(Ph.D. dissertation) Stanford University, Stanford, CA, 2009.
- [26] ASTM A6 / A6M-14, Standard Specification for General Requirements for Rolled Structural Steel Bars, Plates, Shapes, and Sheet Piling, ASTM International, West Conshohocken, PA, 2014.
- [27] L. Kwasnuewski, B. Stojadinovic, S. Goel, SAC Joint Venture Local and Lateral-Torsion Buckling of Wide Flange Beams, SAC Joint Venture: Report SAC BD-99/20, 1999.
- [28] J. Ricles, X. Zhang, L.W. Lu, J. Fisher, Development of Seismic Guidelines for Deep-Column Steel Moment Connections, ATLSS Report no. 04–13, ATLSS Engineering Research Center, Lehigh University, Bethlehem, PA, 2004.
- [29] D.Q. Schweizer, Experimental Investigation of Innovative Seismic Performance Enhancement Techniques for Steel Building Beam to Column Moment Connections, (Thesis) North Carolina State University, Raleigh, NC, 2013.
- [30] J. Newell, C. Uang, Cyclic Behavior of Steel Columns with Combined High Axial Load and Drift Demand, Rep. No. SSRP-06/22, Dept. of Structural Engineering, Univ. of California, San Diego, La Jolla, CA, 2006.
- [31] J. Fogarty, S. El-Tawil, Collapse resistance of steel columns under combined axial and lateral loading, J. Struct. Eng. (2015), 04015091, http://dx.doi.org/10.1061/ (ASCE)ST.1943-541X.0001350.